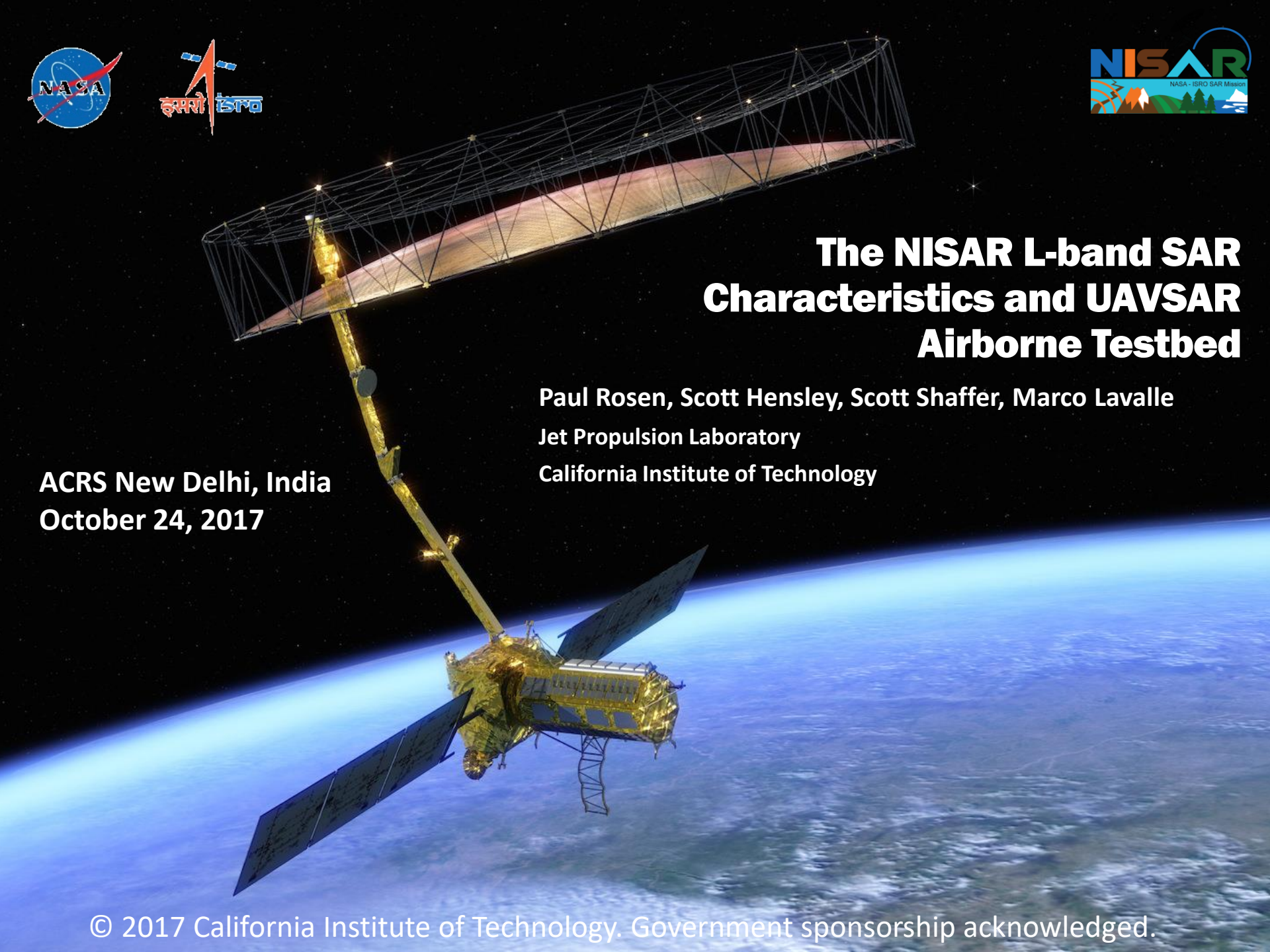

The NISAR L-band SAR Characteristics and UAVSAR Airborne Testbed

Paul Rosen, Scott Hensley, Scott Shaffer, Marco Lavalle
Jet Propulsion Laboratory
California Institute of Technology

ACRS New Delhi, India
October 24, 2017

© 2017 California Institute of Technology. Government sponsorship acknowledged.

NISAR Mission Overview

NISAR Characteristic:	Would Enable:
L-band (24 cm wavelength)	Low temporal decorrelation and foliage penetration
S-band (12 cm wavelength)	Sensitivity to light vegetation
SweepSAR technique with Imaging Swath > 240 km	Global data collection
Polarimetry (Single/Dual/Quad)	Surface characterization and biomass estimation
12-day exact repeat	Rapid Sampling
3 – 10 meters mode-dependent SAR resolution	Small-scale observations
3 years science operations (5 years consumables)	Time-series analysis
Pointing control < 273 arcseconds	Deformation interferometry
Orbit control < 500 meters	Deformation interferometry
> 30% observation duty cycle	Complete land/ice coverage
Left/Right pointing capability	Polar coverage, north and south

NISAR Will Uniquely Capture the Earth in Motion

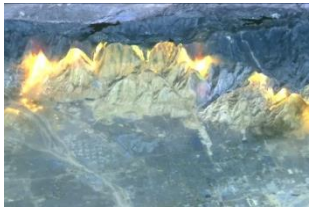

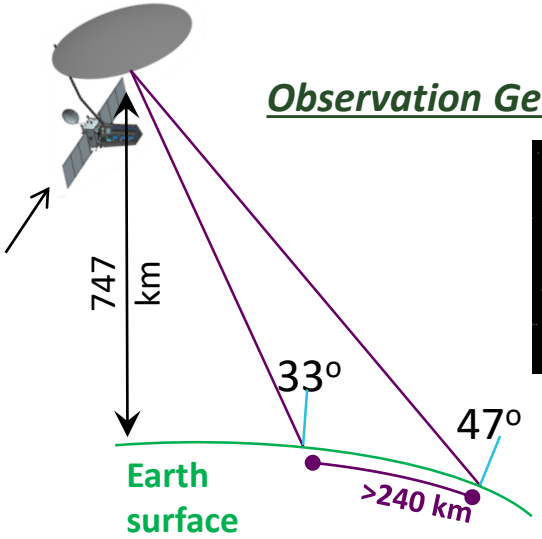

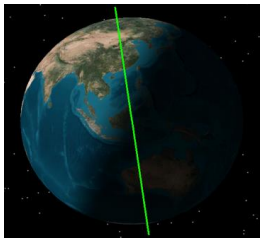

© 2017 California Institute of Technology. Government sponsorship acknowledged.

NISAR Radar Modes

		Science			Performance			
Config. ID	Old Mode #	Primary Science Target	Freq Band	Polarization	BW (MHz)	PRF (Hz)	PW [∝sec]	Swath [km]
128	L1	Background Land	L	DP HH/HV	20+5	1650	25	242
129		Background Land Soil Moisture	L	QQ	20+5	1650	25	242
130		Background Land Soil Moisture Hi Pwr	L	QQ	20+5	1650	20	242
131	L2	Land Ice	L	SP HH	80	1650	40	121
132		Land Ice Low Res	L	SP HH	40+5	1650	45	242
133		Low Data Rate Study Mode SinglePol	L	SP HH	20+5	1650	25	242
134	L3	Sea Ice Dynamics	L	SP VV	5	1600	25	242
135		Open Ocean	L	QD HH/VV	5+5	1650	20	242
136	L4	India Land Characterization	L	DP VV/VH	20+5	1650	25	242
137	L5	Urban Areas, Himalayas	L	DP HH/HV	40+5	1650	45	242
138		Urban Areas, Himalayas SM	L	QQ	40+5	1650	45	242
139		Urban Areas, Himalayas SM Hi Pwr	L	QQ	40+5	1650	40	242
140	L6	US Agriculture, India Agriculture	L	QP HH/HV/VH/VV	40+5	1600*	45	242
141	LX	US Agriculture, India Agriculture Low Res	L	QP HH/HV/VH/VV	20+5	1600*	45	242
142	L7	Experimental CP mode	L	CP RH/RV	20+20	1650	40	242
143	L8	Experimental QQ mode	L	QQ	20+20	1650	20	242
144	L9	Experimental SP mode	L	SP HH	80	1650	20	242
145		ISRO Ice/sea-ice	L	DP VV/VH	5	1650	25	242
146		ISRO Ice/sea-ice alternate	L	QD HH/VV	5	1650	25	242
64	S1	Solid Earth/Ice/Veg/Coast/Bathym	S	Quasi-Quad	37.5	2200	10+10	244
65	S2	Ecosystem/Coastal Ocean/Cryosphere	S	DP HH/HV	10	2200	25	244
66	S3	Agriculture/Sea Ice	S	CP RH/RV	25	2200	25	244
67	S4	Glacial Ice-High Res	S	CP RH/RV	37.5	2200	25	244
68	SX	New mode	S	DP HH/HV	37.5	2200	25	244
69	S5	Deformation	S	SP HH (or SP VV)	25	2200	25	244
70	S6	Deformation-Max Res	S	SP HH (or SP VV)	75	2200	25	244

© 2017 California Institute of Technology. Government sponsorship acknowledged.

NISAR Joint Radar Modes

		Science			Performance			
Config. ID	Old Mode #	Primary Science Target	Freq Band	Polarization	BW (MHz)	PRF (Hz)	PW [∝sec]	Swath [km]
192	**L1+S3**	Systematic Coverage	L+S	DP HH/HV CP RH/RV	20+5 25	1910^	25 25	242 244
193	**L1+S4**	Systematic Coverage & Deformation	L+S	DP HH/HV DP HH/HV	20+5 37.5	1910^	25 25	242 244
194	**L1+S5**	Coastal-Mudbank (wet soil ????)	L+S	DP HH/HV SP HH (or SP VV)	20+5 25	1910^	25 25	242 244
195	**L3+S2**	Ocean	L+S	SP VV DP VV/VH	5 10	1910^	25 25	242 244
196	**L4+S3**	Sea Ice Types	L+S	L: DP VV/VH S: CP RH/RV	20+5 25	1910^	25^ 25	242 244
197	**L5+S4**	Glacial Ice-Himalayas	L+S	L: DP HH/HV S: CP/RH/RV	40+5 37.5	1910^	45^ 25	242 244
198	**L5+S6**	High-Res Deformation(Disaster/Urgent Response)	L+S	L: DP HH/HV S: SP HH (or SP VV)	40+5 75	1910^	45^ 25	242 244
199	**L6+S3**	India Agriculture	L+S	L: QP HH/HV/VH/VV S: CP RH/RV	40+5 25	1550*^ 3100	45^ 10'	242 244
200	**L6+SX**	Coastal Land	L+S	L: QP HH/HV/VH/VV S: DP HH/HV	40+5 37.5	1550*^ 3100	45^ 10'	242 244
201	**LX+S3**	Coastal X	L+S	L: QP HH/HV/VH/VV S: CP HH/HV	20+5 25	1550*^ 3100	45^ 10'	242 244
202	**LX+SX**	Coastal X	L+S	L: QP HH/HV/VH/VV S: DP HH/HV	20+5	1550*^ 3100	45^ 10'	242 244
203	**L?+S3**	ISRO Ice/sea-ice	L+S	DP VV/VH CP RH/RV	5 25	1910^	25 25	242 244
204	**L?+S2**	ISRO Ice/sea-ice joint Alternate	L+S	DP VV/VH DP VV/VH	5 10	1910^	25 25	242 244

© 2017 California Institute of Technology. Government sponsorship acknowledged.

NISAR Instrument Overview

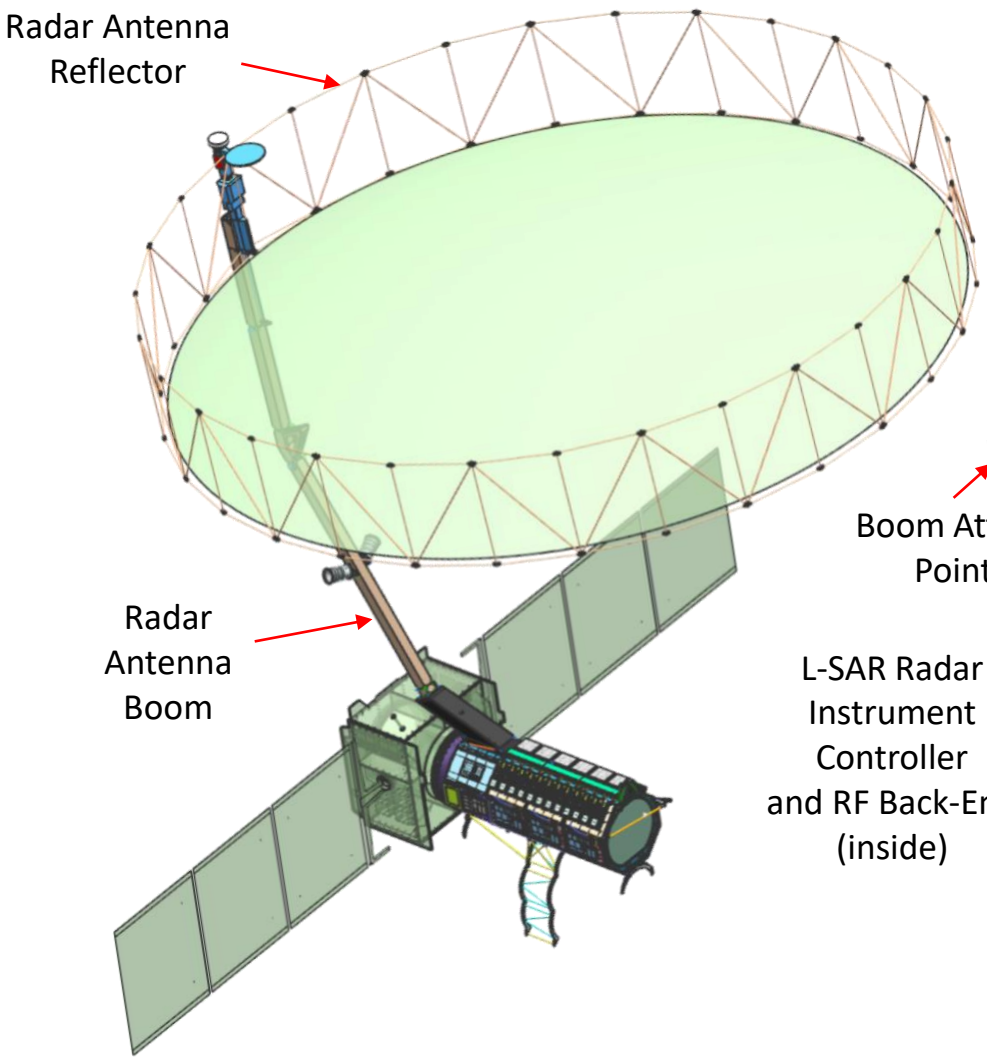

Instrument Subsystems:

- L-Band SAR (JPL)
- S-Band SAR (ISRO)
- Instrument Structure (JPL)
- Radar Antenna (JPL)

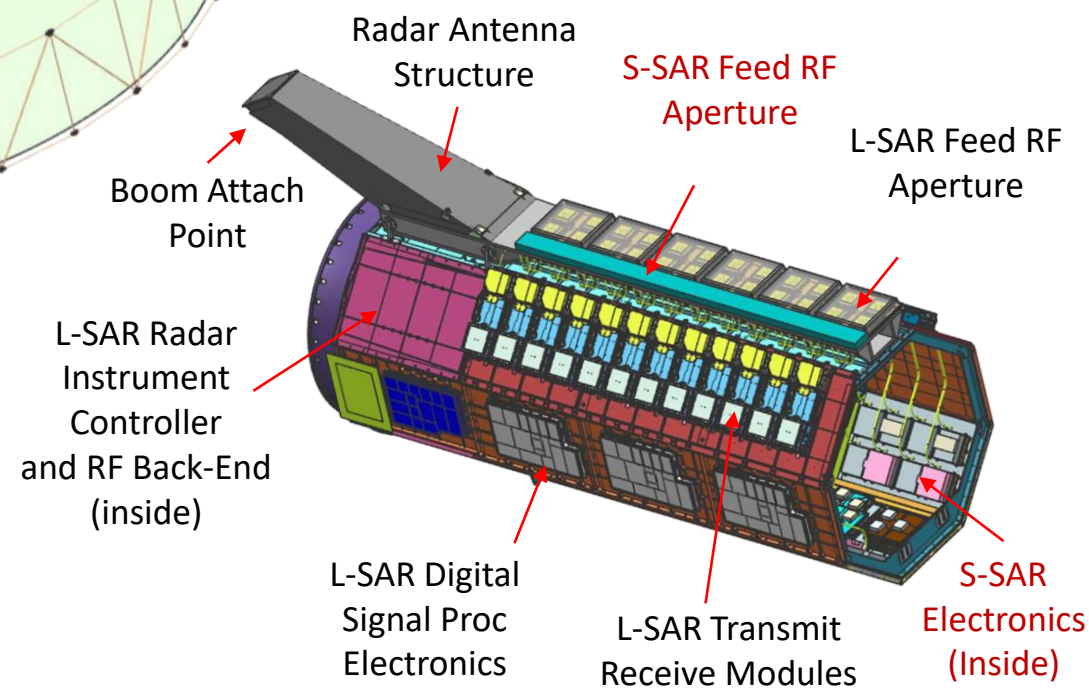

Instrument Structure also houses GPS unit and Solid State Recorder

© 2017 California Institute of Technology. Government sponsorship acknowledged.

Progress in Development Phase C
L-band SAR Hardware (1/2)

EM Waveform Generator

EM Up Converter Driver

EM Frequency Synthesizer

EM RBE-PCU

EM RBE Stack

EM TRM-ESS

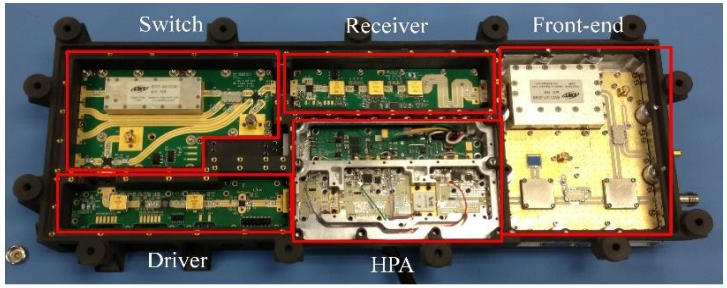

TRM Pathfinder EM

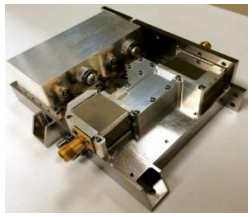

EM Front-End Subassembly (FES)

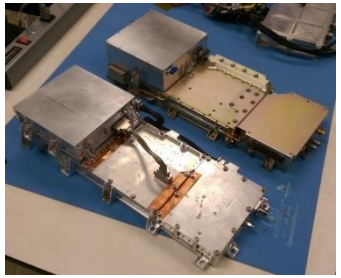

Prototype and Pathfinder TRMs

EM RIC-CTB

EM RIC-SIF

RIC- RAD750 Qual Model

EM RIC-HKT

EM RIC-PCU

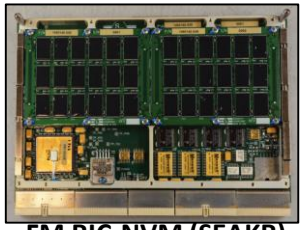

FM RIC-NVM (SEAKR)

Digital Signal Processor

EM QFSP

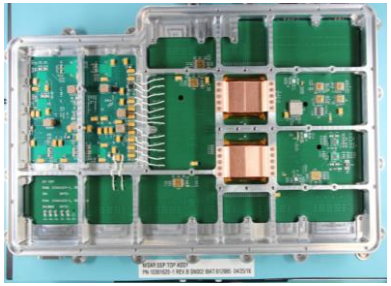

EM SSP

© 2017 California Institute of Technology. Government sponsorship acknowledged.

Progress in Development Phase C
L-band SAR Hardware (2/2)

Boom and Hinge Development Hardware

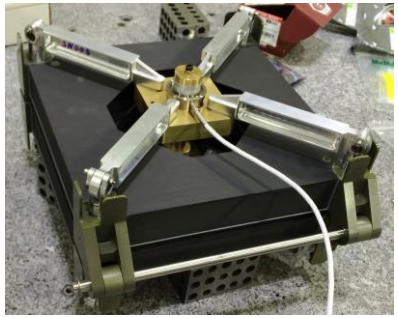

10" Development Boom Stability Test

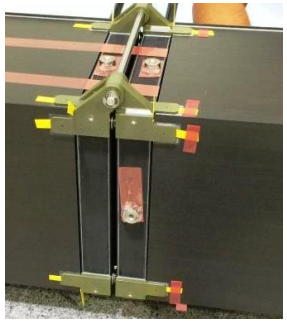

7" Prototype Boom/Hinge in fabrication

L-FRAP Feed Tile Development Hardware

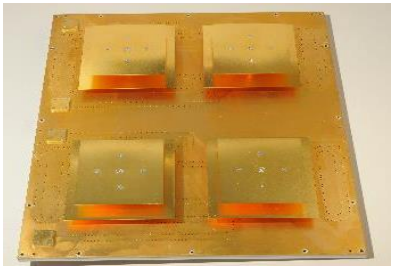

Feed Tile EM (without radome)

Hinge Deploy & Latching H/W

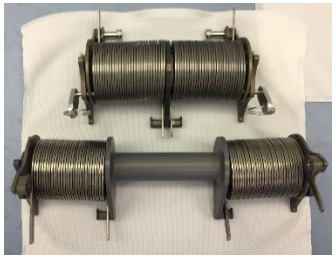

PT Spring Assemblies

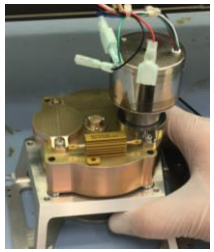

Boom Actuator PT

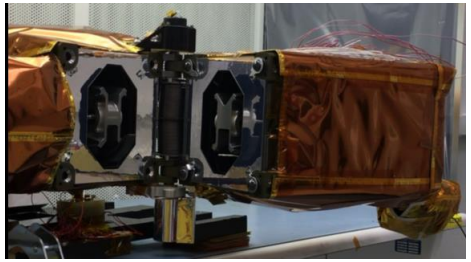

Prototype 7" Spring/Damper Deploy Test

Feed Array EM in Test

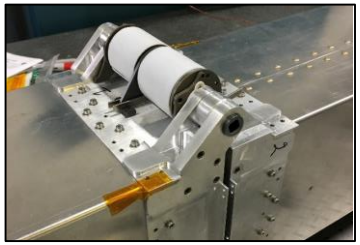

Hinge Spring Cartridge Torque Test

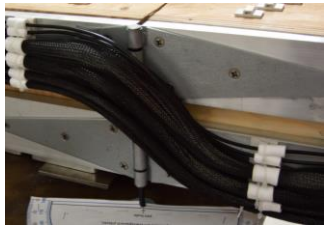

Boom Harness Torque Test

© 2017 California Institute of Technology. Government sponsorship acknowledged.

Front-end Radiating Aperture
S-band Development and Joint L+S compatibility

L-band aperture

L+S structure

© 2017 California Institute of Technology. Government sponsorship acknowledged.

How the L- and S-band radars coordinate observations

- The L-band and S-band radars uses a set of upload-able tables to control radar operations
- Consecutive ***Observations*** with the same start time are grouped into a ***Datatake*** and collected back-to-back with seamless transitions between them
- Each Datatake has a Pre- and Post-take for calibration and at least one or more observations

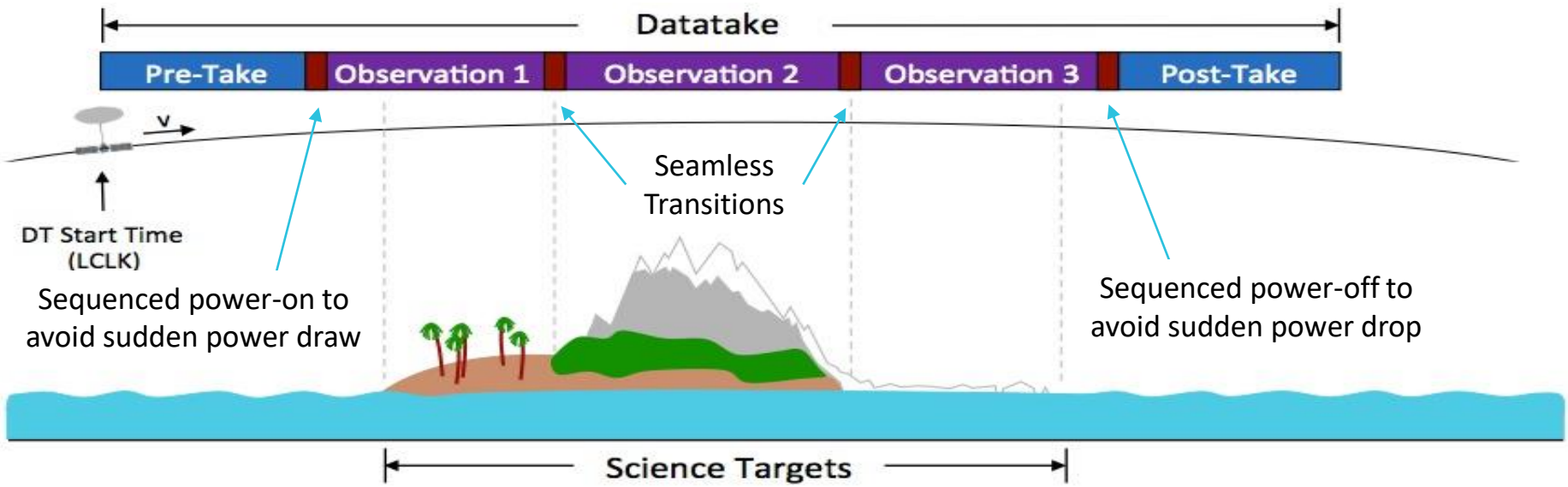

© 2017 California Institute of Technology. Government sponsorship acknowledged.

How the L- and S-band radars coordinate timing

- **Joint Data Take Timing Synchronization**
  - To avoid mutual interference during joint operations, transmit events are synchronized
  - L-SAR generates a Timing Reference Pulse and a Global Blanking Pulse and forwards them to the S-SAR electronics to ensure that the transmit events occur in sync
  - L-SAR transmits a digital message to the S-SAR to indicate pulse count, radar clock time, and other parameters to help align the operations of the two radars
  - S-SAR uses the L-SAR STALO and timing signals to derive its pulse timing signals

- **Datatake Power Sequencing**
  - Because of power system constraints, the transitions from idle to transmit and transmit to idle must be sequenced on to prevent transients on the bus
  - S-SAR also does power sequence, but offset from L-SAR to minimize transients on the power bus

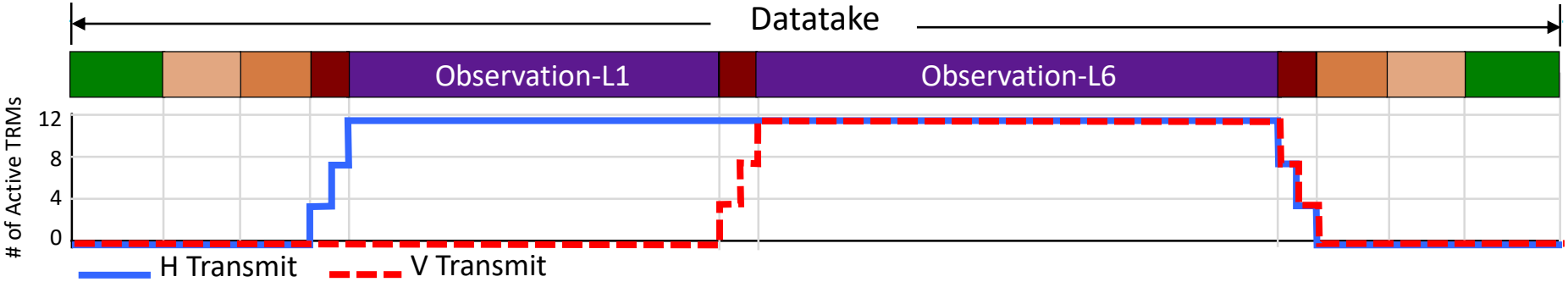

© 2017 California Institute of Technology. Government sponsorship acknowledged.

L-SAR / S-SAR electrical interfaces are simple and robust

- To ensure proper timing during joint radar operations, four signals are generated by the L-SAR radar electronics and provided to S-SAR. These signals consist of:
  - **Frequency Reference**: 10 MHz StaLO RF signal to derive timing signals (50ohm coax)
  - **Global Blanking Pulse**: Pulsed RS422 signal to synchronize transmit events
  - **Radar Timing Reference**: Pulsed RS422 to serve as a precise time marker
  - **Radar Serial Message**: Asynchronous serial message containing radar mode, L-SAR clock time, L-SAR pulse count, GPS time and position, etc.
- S-SAR uses L-SAR StaLO and timing signals to derive its pulse timing signals for any datatake that contains at least one joint observation

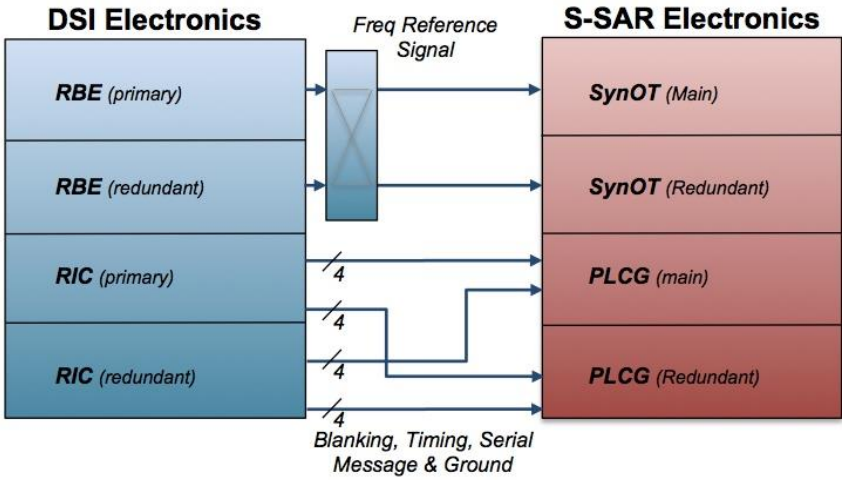

© 2017 California Institute of Technology. Government sponsorship acknowledged.

UAVSAR: NASA's Multi-Frequency Reconfigurable Imaging Radar Testbed

Used to develop, validate, and improve new radar technologies and algorithms for modeling geophysical phenomena for future Earth-observing satellite missions.

L-band polarimetry for land use and classification

L-band single-pass polarimetric interferometry to provide vertical structure of ice and vegetation

L-band repeat-pass interferometry

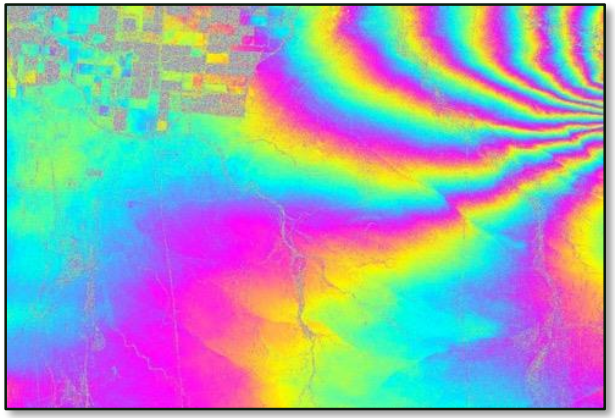

Mexicali earthquake deformation captured by UAVSAR using data acquired on October 21, 2009 and April 13, 2010.

Ka-band single-pass InSAR for observing glacier and land ice topography

P-band POLSAR (AirMOSS) for measuring subsurface and subcanopy soil moisture

Other Configurations

© 2017 California Institute of Technology. Government sponsorship acknowledged.

UAVSAR L-band Operational Parameters

Parameter	Value
Frequency	L-Band 1217.5 to 1297.5 MHz (80 MHz)
Polarization	Full Quad-Polarization
Resolution	1.67 m Range, 0.8 m Azimuth
Range Swath	22 km (13.2 miles)
Look Angle	25° - 65°
Azimuth Steering Range	±25°
Platform	Gulfstream III
Nominal Altitude	13.7 km (45,000 ft) – GPS Altitude
Nominal Ground Speed	210 m/s (~420 knots)
Nominal Flight Duration	6 hours (8-15 Flight Lines ~ 150-300 km)

© 2017 California Institute of Technology. Government sponsorship acknowledged.

UAVSAR Flight Track Repeatability on G-III

Repeated aircraft tracks (blue lines) are within the 10 m tube in order to extract the centimeter-level changes in deformation from the target site.

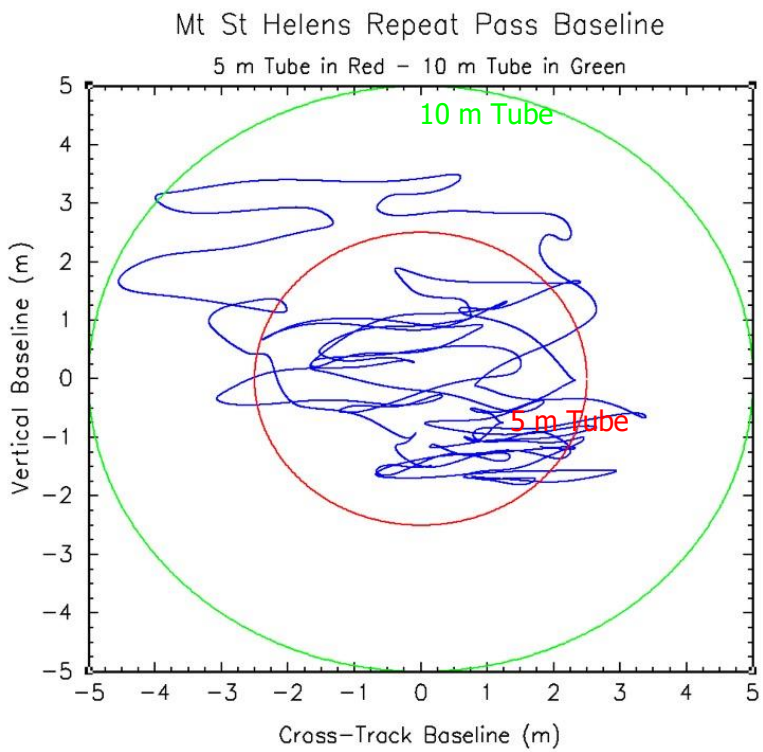

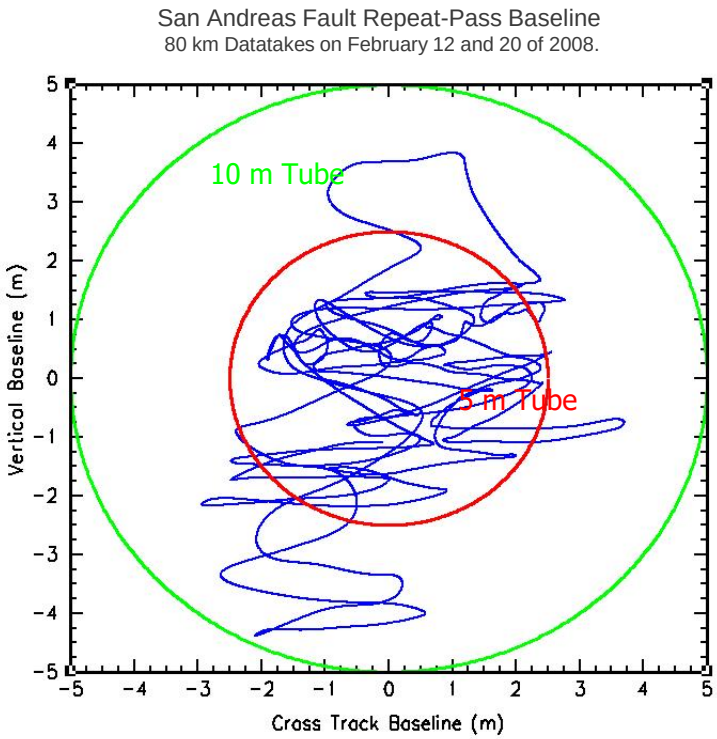

UAVSAR
Uninhabited Aerial Vehicle Synthetic Aperture Radar

© 2017 California Institute of Technology. Government sponsorship acknowledged.

UAVSAR data collected since 2008

Acquisition (flown)

Successful Data Takes	5,411
Successful Kilometers*	726,875
Successful Raw Data Volume (GB)	137,418
Aborted Data Takes	165
Data Flights	553

*Calculated using length from planned swaths

UAVSAR
Uninhabited Aerial Vehicle Synthetic Aperture Radar

Successful Data Takes by Discipline

Applied Sciences	839
Biodiversity	3
Cryosphere	465
Engineering	0
Hydrology	386
Land Cover Land Use Change	39
Oceanography	36
Rapid Response	27
Solid Earth (Earthquakes)	1,755
Solid Earth (Other deformations)	532
Solid Earth (Volcanoes)	947
Space Archaeology	12
Terrestrial Ecology	370

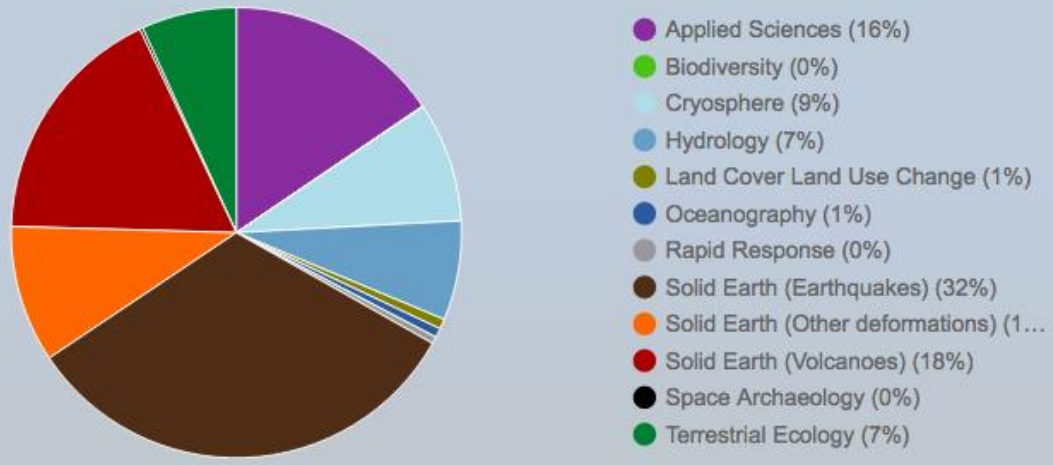

© 2017 California Institute of Technology. Government sponsorship acknowledged.

Classification of Scattering Mechanism with Polarimetry

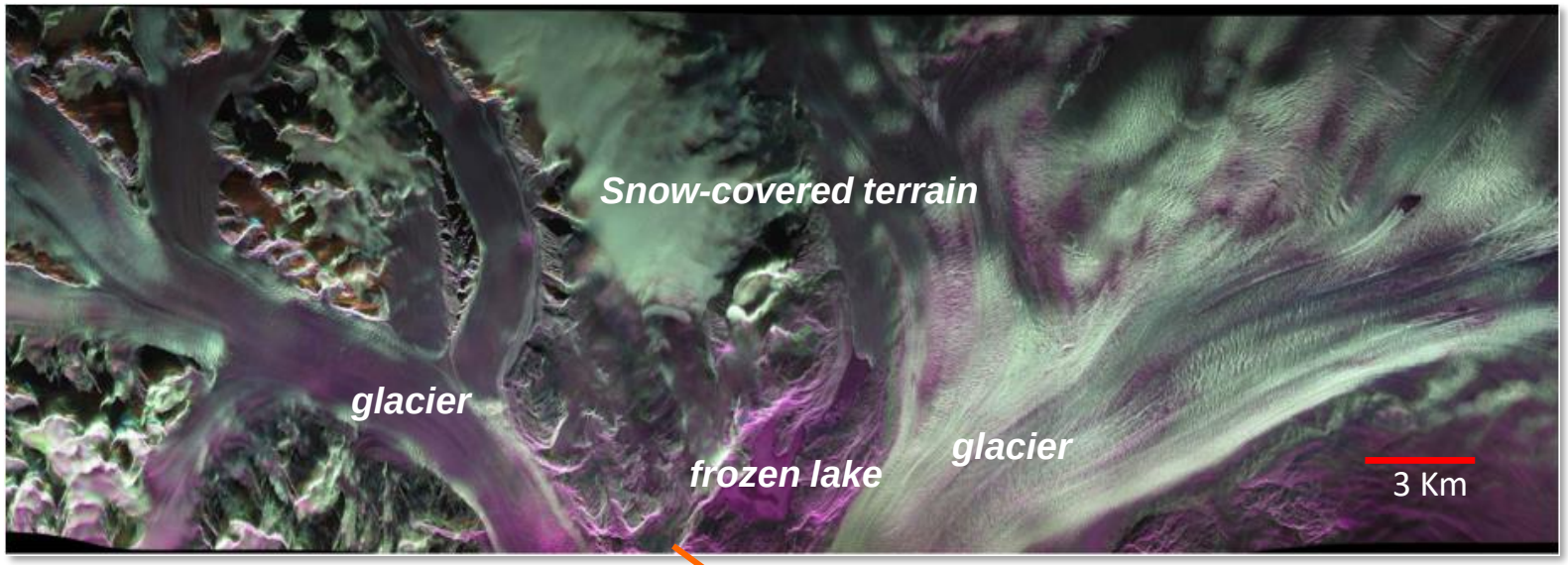

Kangerlugssuaq Glacier in Greenland

UAVSAR
Uninhabited Aerial Vehicle Synthetic Aperture Radar

© 2017 California Institute of Technology. Government sponsorship acknowledged.

Lanin Glacier Deformation

Climate-induced glacier retreat has important consequences for water resource management in Andean countries.

UAVSAR
Uninhabited Aerial Vehicle Synthetic Aperture Radar

USGS, NASA, and the Chilean Air Force collaboration to **assess the health of Chile's glacier resources.**

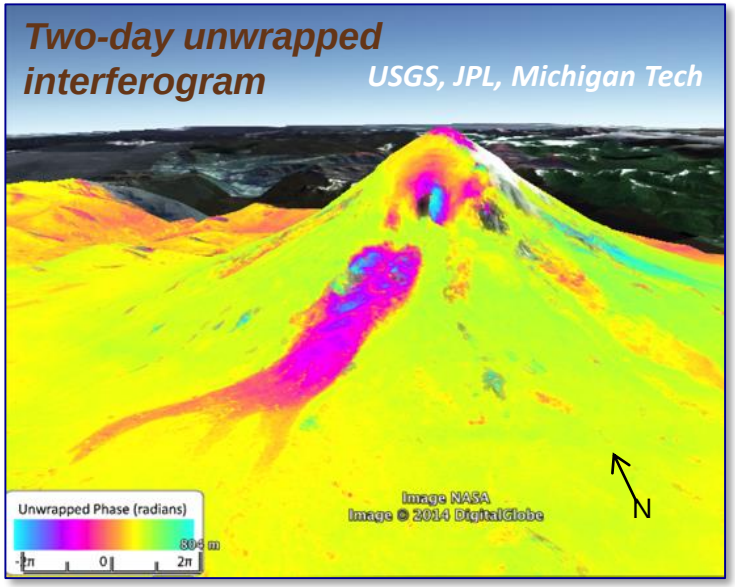

In March 2013, UAVSAR imaged 4 glaciers at the Chilean-Argentinian border to **provide a unique view of their short-timescale (< 4 day) temporal dynamics**. Results indicate:

- Significantly faster velocities;
- More widespread activity.

Ice velocity fields derived from UAVSAR InSAR products are being integrated with remote sensing and ground data maintained by Chilean institutions:

- Lidar
- GASS instruments: Glacier Ablation Sensor Systems

NISAR
NASA - ISRO SAR Mission

© 2017 California Institute of Technology. Government sponsorship acknowledged.

L-band Sea Ice Data at Beaufort Sea

October 6, 2016

Provided by:
Scott Hensley
and Yunling Lou

UAVSAR
Uninhabited Aerial Vehicle Synthetic Aperture Radar

20 km

35 km

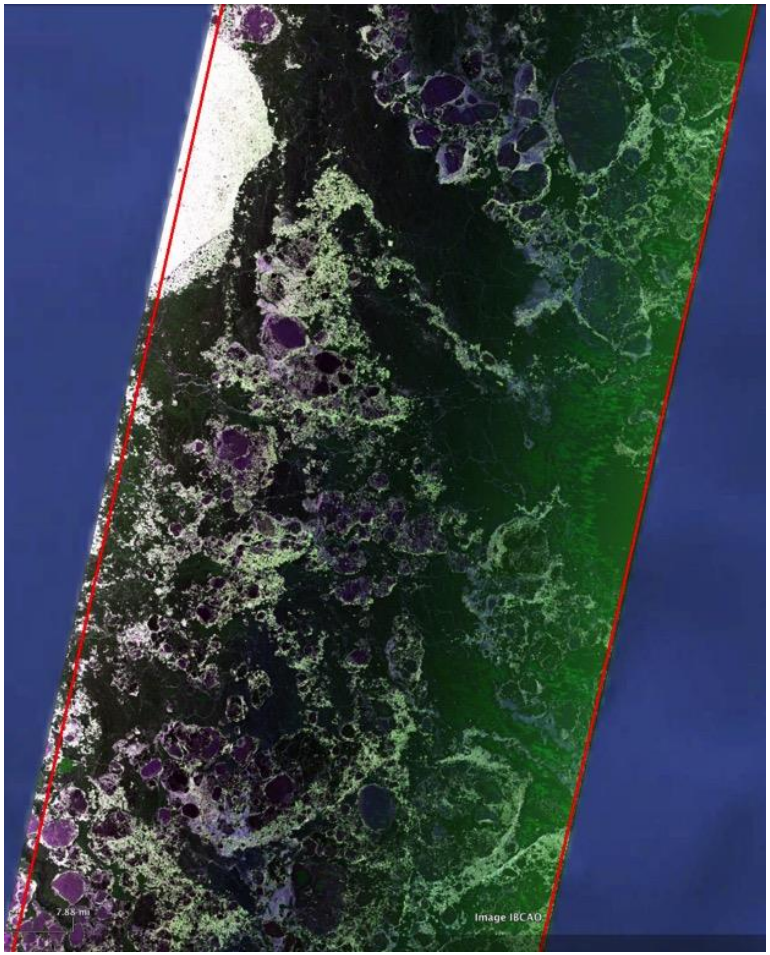

N

HH=red, VV=blue and HV=green

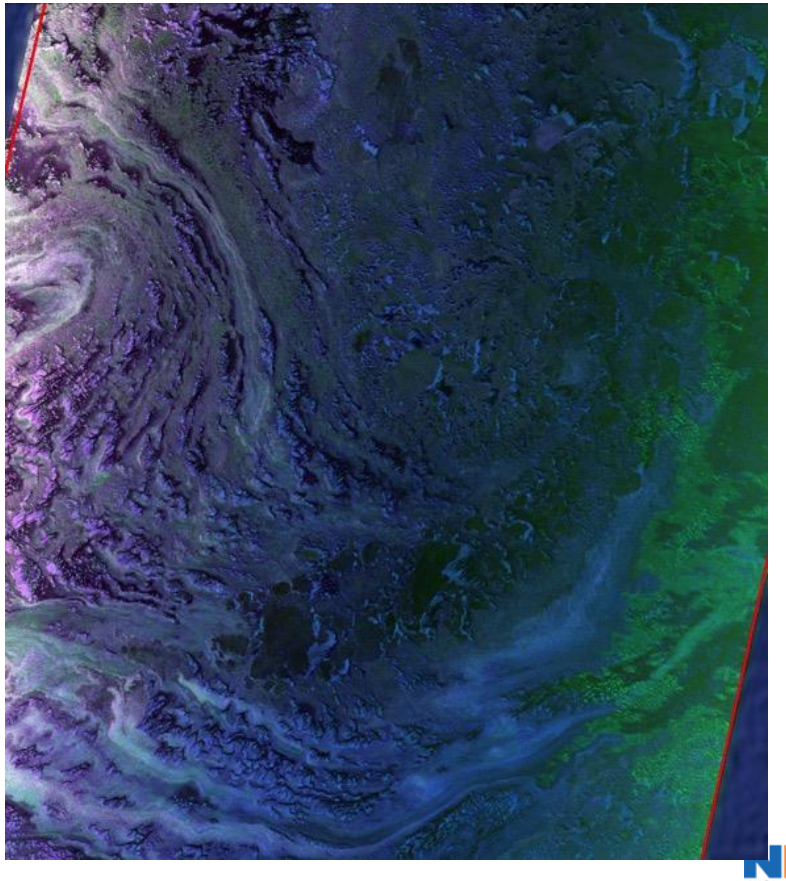

NISAR
NASA - ISRO SAR Mission

© 2017 California Institute of Technology. Government sponsorship acknowledged.

Oil Slick Detection Off Louisiana Coast

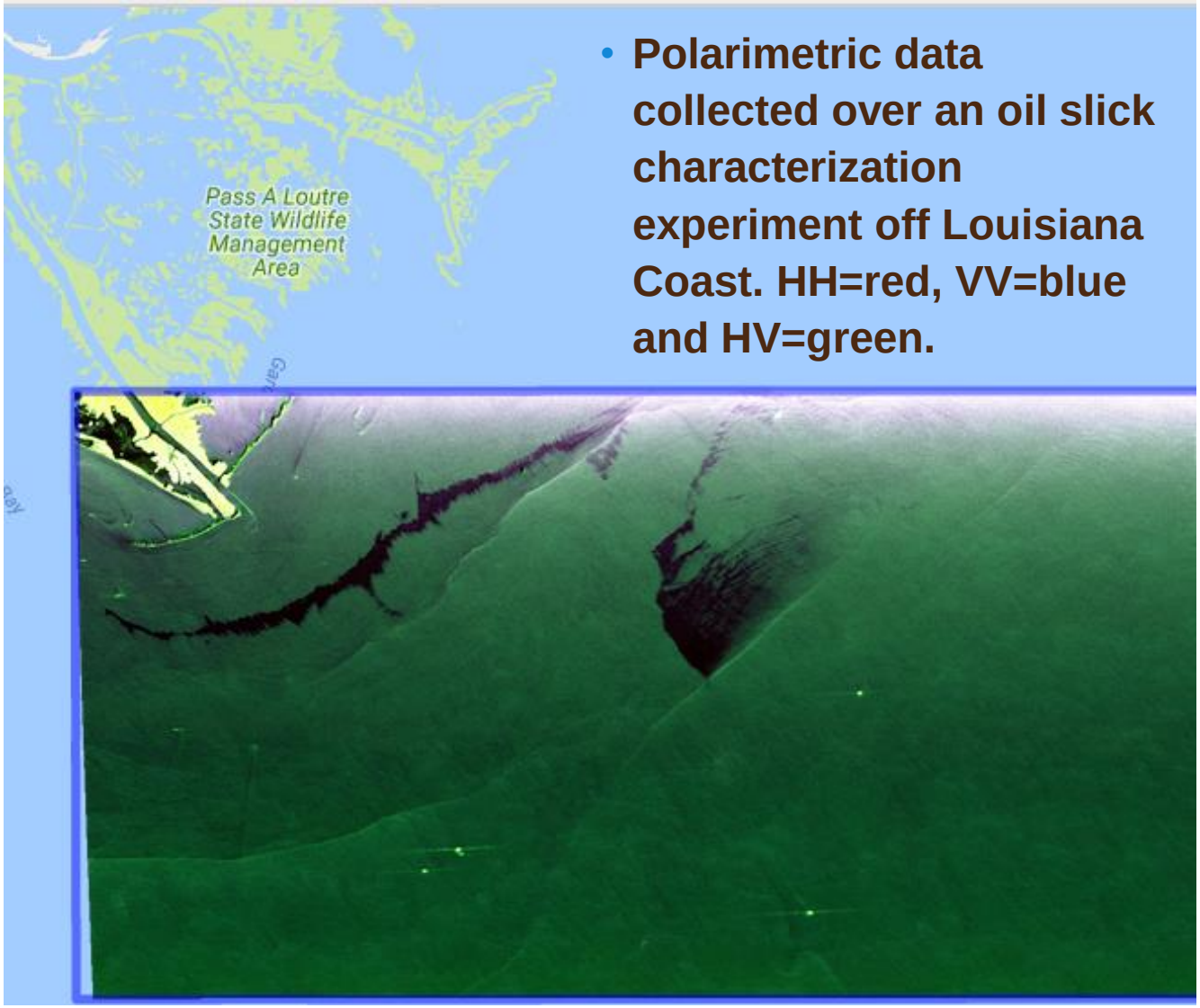

- Polarimetric data collected over an oil slick characterization experiment off Louisiana Coast. HH=red, VV=blue and HV=green.

Provided by:
Scott Hensley
and Yunling Lou

© 2017 California Institute of Technology. Government sponsorship acknowledged.

Mapping Amazon Wetlands with Polarimetry

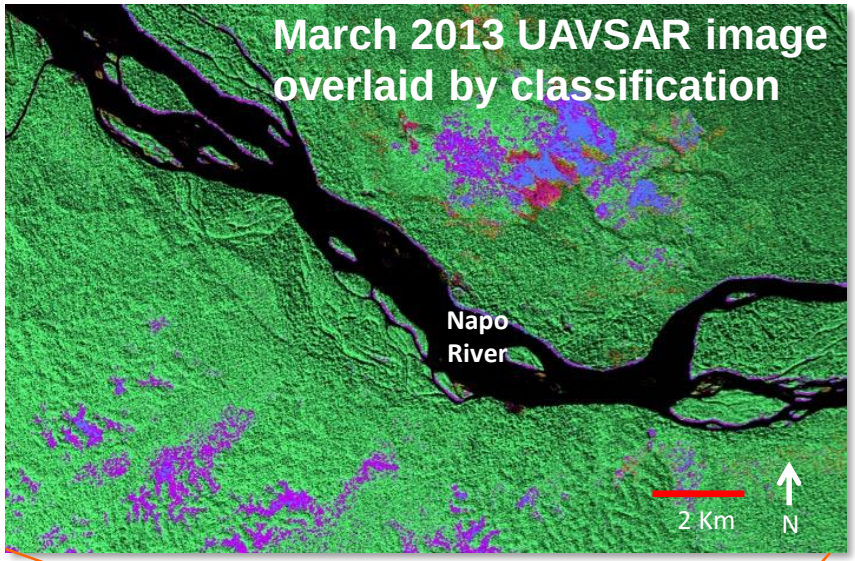

Methane emissions play a critical role in anthropogenic climate forcing but are poorly resolved globally. **Large uncertainties are attributed to tropical wetlands where inundation duration drives methane production**. Polarimetric UAVSAR imagery can be used to classify the inundation state more robustly than data by other sensors and at high resolution (6x6 meters).

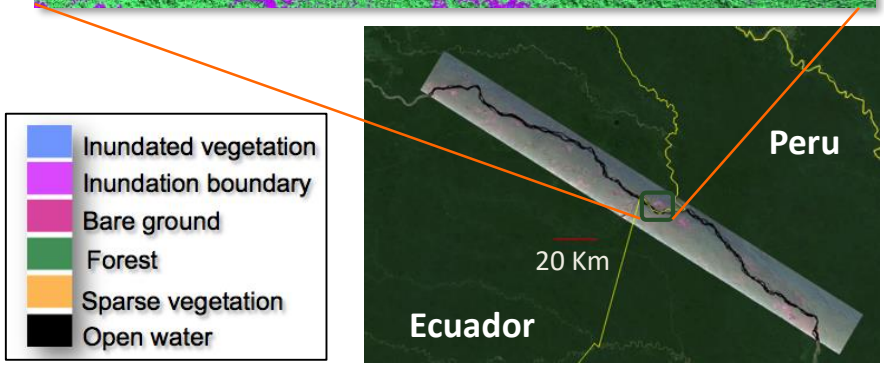

Fine-resolution inundation maps are being produced from UAVSAR data acquired in South America in 2013

UAVSAR
Uninhabited Aerial Vehicle Synthetic Aperture Radar

© 2017 California Institute of Technology. Government sponsorship acknowledged.

Deformation at Kilauea Volcano

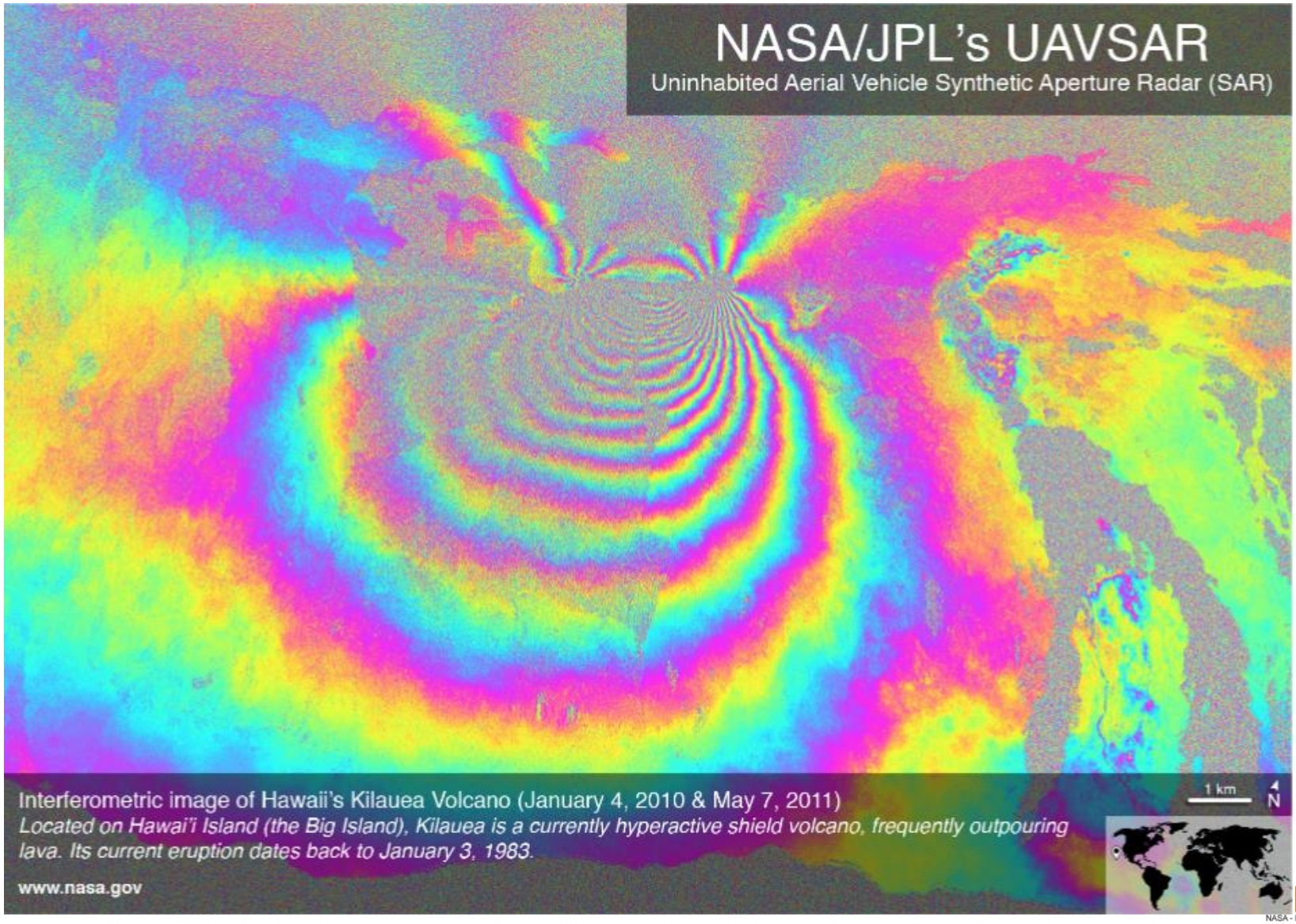

© 2017 California Institute of Technology. Government sponsorship acknowledged.

SLC Stack Processing

- Stack of Mauna Loa Volcano in the Big Island of Hawaii
  - 35 time steps dating back to January 2010
  - Captures deformation signature between November 2013 & October 2016

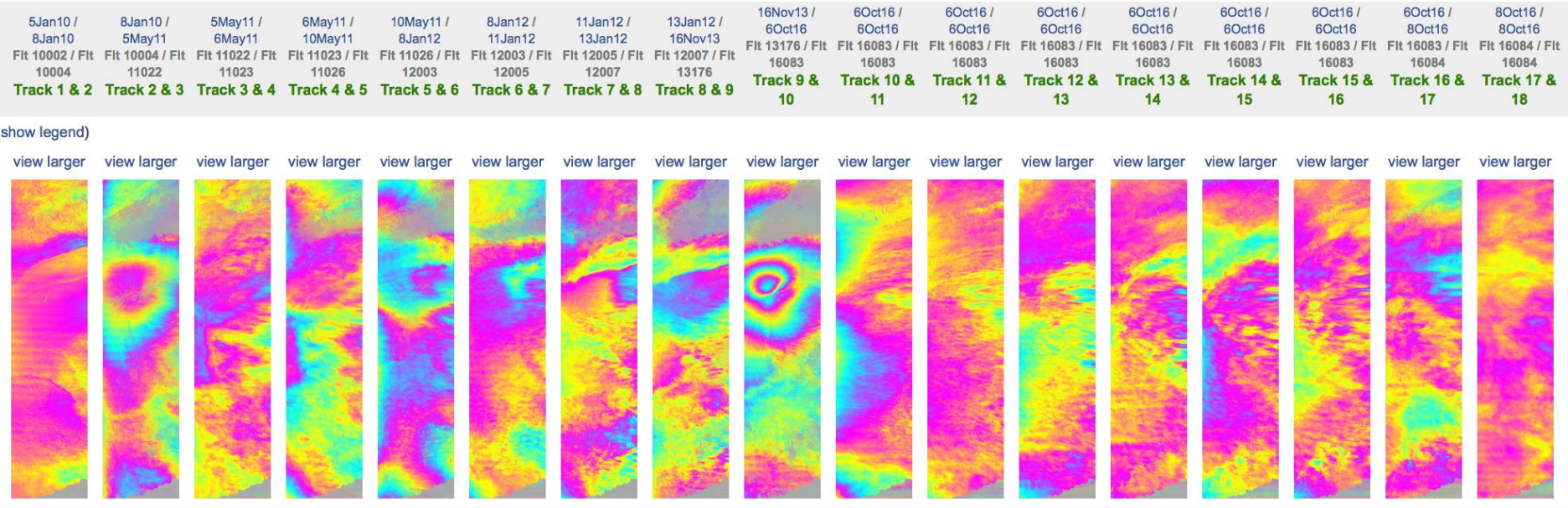

UAVSAR
Uninhabited Aerial Vehicle Synthetic Aperture Radar

NISAR
NASA - ISRO SAR Mission

© 2017 California Institute of Technology. Government sponsorship acknowledged.

UAVSAR Studies Sacramento Delta, California
Multi-year time series every 6 weeks

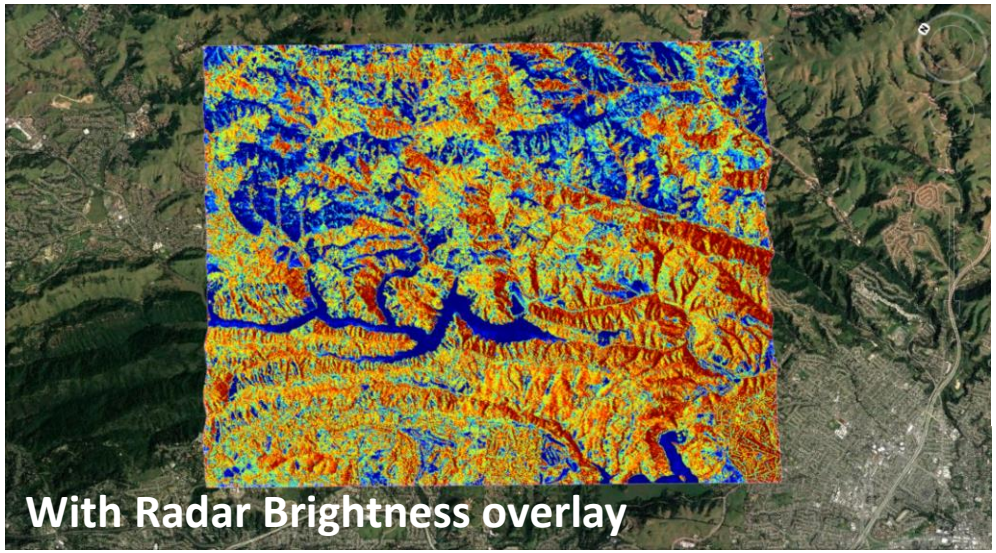

- Focus polarimetric SLCs using UAVSAR processor
- Co-register SLCs using *Interferometric SAR Scientific Computing Environment (ISCE)*
- Create intensity image from SLC
- Geocode the image
- Calculate HV beta-nought
- Study variability

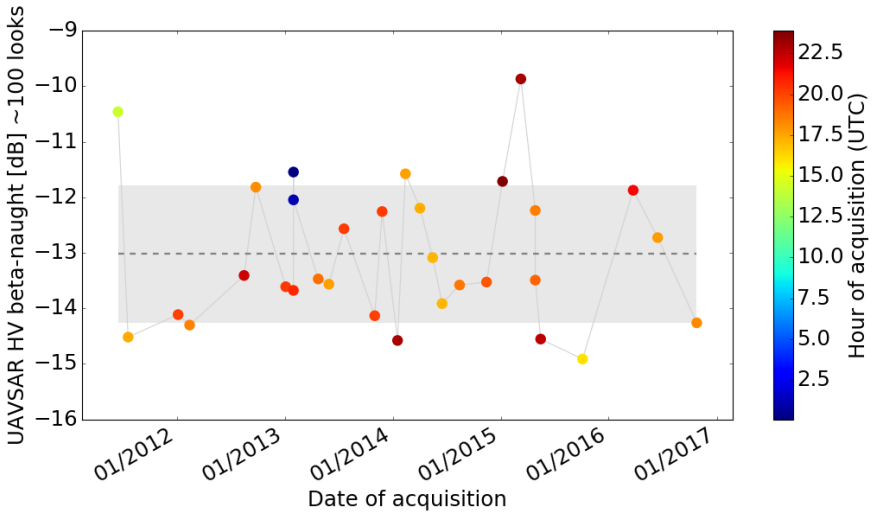

UAVSAR
Uninhabited Aerial Vehicle Synthetic Aperture Radar

© 2017 California Institute of Technology. Government sponsorship acknowledged.

UAVSAR Radiometric Time Series
Sacramento Delta, California

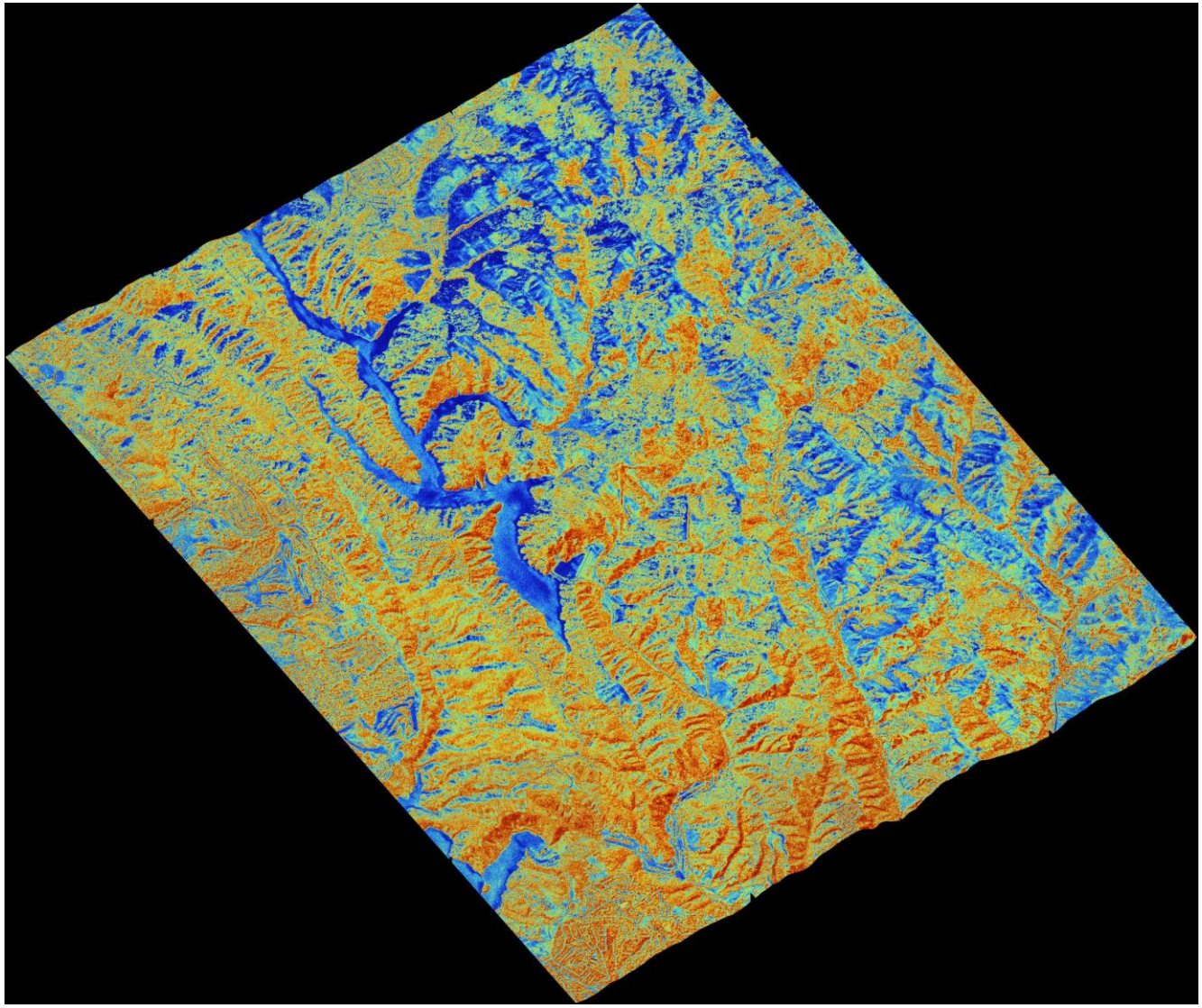

© 2017 California Institute of Technology. Government sponsorship acknowledged.

Conclusion

- NISAR is currently in “development” phase (C)
  - Key electronics fabricated to EM level
  - Major procurements executed
  - L- and S-band SAR instruments are being built for joint operations
- Joint L&S band SAR observations planned over extensive areas surrounding India, Indonesia, and the polar regions,
  - Serving as a natural laboratory for dual-band phenomenology and science
- ISRO Airborne L&S band SAR will provide science community with an multidisciplinary science data set to prepare for NISAR
  - First flights in June 2017 – preliminary results demonstrate functionality and show some interesting phenomenological frequency-dependent effects
- Discussions within the joint science team for conducting a joint campaign with UAVSAR in India in 2019

© 2017 California Institute of Technology. Government sponsorship acknowledged.

Backup